THE JOURNAL OF BIOLOGICAL CHEMISTRY
Vol. 279, No. 48, Issue of November 26, pp. 49902–49909, 2004
Printed in U.S.A.

Phosphorylation of the Sarcoplasmic Reticulum Ca^{2+}-ATPase from ATP and ATP Analogs Studied by Infrared Spectroscopy*

Received for publication, July 16, 2004, and in revised form, September 7, 2004
Published, JBC Papers in Press, September 20, 2004, DOI 10.1074/jbc.M408062200

Man Liu‡§ and Andreas Barth¶

From the ‡Institut für Biophysik, Johann Wolfgang Goethe-Universität, 60596 Frankfurt am Main, Germany and ¶Department of Biochemistry and Biophysics, The Arrhenius Laboratories for Natural Sciences, Stockholm University, S-106 91 Stockholm, Sweden

Phosphorylation of the sarcoplasmic reticulum Ca^{2+}-ATPase (SERCA1a) was studied with time-resolved Fourier transform infrared spectroscopy. ATP and ATP analogs (ITP, 2′- and 3′-dATP) were used to study the effect of the adenine ring and the ribose hydroxyl groups on ATPase phosphorylation. All modifications of ATP altered conformational changes and phosphorylation kinetics. The differences compared with ATP increased in the following order: 3′-dATP > ITP > 2′-dATP. Enzyme phosphorylation with ITP results in larger absorbance changes in the amide I region, indicating larger conformational changes of the Ca^{2+}-ATPase. The respective absorbance changes obtained with 3′-dATP are significantly different from the others with different band positions and amplitudes in the amide I region, indicating different conformational changes of the protein backbone. ATPase phosphorylation with 3′-dATP is also much (~30 times) slower than with ATP. Our results indicate that modifications to functional groups of ATP (the ribose 2′- and 3′-OH and the amino group in the adenine ring) affect γ-phosphate transfer to the phosphorylation site of the Ca^{2+}-ATPase by changing the extent of conformational change and the phosphorylation rate. ADP binding to the ADP-sensitive phosphoenzyme (Ca_2E1P) stabilizes the closed conformation of Ca_2E1P.

In skeletal muscle cells the Ca^{2+}-ATPase of sarcoplasmic reticulum (SR)[1] pumps Ca^{2+} actively from the cytoplasm into the SR lumen (1–6). ATP hydrolysis supplies the energy for Ca^{2+} transport. In the reaction cycle of Ca^{2+} transfer, the ATPase undergoes conformational changes and forms several intermediates including Ca_2E1 (the calcium-ATPase complex with high affinity to Ca^{2+}), Ca_2E1ATP (the calcium-ATP-ATPase complex), Ca_2E1P (the ADP-sensitive phosphoenzyme), E2P (the ADP-insensitive phosphoenzyme), and E2 (the calcium-free ATPase with low affinity to Ca^{2+}).

Crystal structures of the SR Ca^{2+}-ATPase (7–10) show that the enzyme has two regions, the transmembrane region and the cytoplasmic region. The cytoplasmic region consists of three globular domains: nucleotide domain (N domain), phosphorylation domain (P domain), and actuator or anchor domain (A domain), which are connected by hinge regions. The adenosine part of ATP binds to the N domain (11), and the phosphorylated residue Asp-351 is located in the P domain (7). It has been proposed that the structures of Ca_2E1ATP and of Ca_2E1P are similar, indicated by similar infrared spectra of ATP binding and Ca_2E1P formation (12) and by a proteolysis study (13). Recently crystal structures of the complex Ca_2E1AMPPCP and the Ca_2E1P analogue Ca_2E1ADP:AlF_4^- were obtained (9, 10). They are almost identical and show a compact arrangement of domains. The aim of this work is to study the conformational difference between the Ca_2E1ATP and Ca_2E1P state with Fourier transform infrared (FTIR) spectroscopy.

Infrared spectroscopy (14–18) has several advantages for elucidating the molecular mechanism of proteins, such as high time resolution, universal applicability from small soluble proteins to large membrane proteins, and high molecular information content combined with a sensitivity high enough to detect a change in the environment around a single atom of a large protein. These properties make this method very useful to obtain information on enzyme-substrate recognition (18–21). FTIR spectroscopy (22–27) can provide potent dynamic and structural information, which sheds light on interactions occurring between enzyme and substrate during the catalytic process. In our previous work (21, 28, 29), various nucleotides have been used to probe interactions between nucleotides and the SR Ca^{2+}-ATPase in the nucleotide binding reaction with FTIR spectroscopy, and characteristic binding modes for each nucleotide have been concluded.

Here we investigate enzyme phosphorylation with ATP and ATP analogs inosine 5′-triphosphate (ITP) and 2′- and 3′-dATP to identify important functional groups of ATP for ATPase phosphorylation. The analogs differ from ATP at individual functional groups, which allows us to study the impact of these groups on the conformational change in the phosphorylation reaction (Ca_2E1ATP → Ca_2E1P). Photolabile derivatives, *i.e.* P^3-1-(2-nitrophenyl)ethyl nucleotides (caged nucleotides) (30), were used to trigger the protein reaction directly in the infrared cuvette in order to detect the small infrared absorbance changes associated with phosphorylation of the Ca^{2+}-ATPase.

* This work was supported by Deutsche Forschungsgemeinschaft Grants Ba1887/2-1 and Ma1054/18-3, Vetenskapsrådet, and Knut och Alice Wallenbergs Stiftelse. The costs of publication of this article were defrayed in part by the payment of page charges. This article must therefore be hereby marked "*advertisement*" in accordance with 18 U.S.C. Section 1734 solely to indicate this fact.

§ To whom correspondence should be addressed. Tel.: 46-8-163529; Fax: 46-8-155597; E-mail: liu@dbb.su.se.

[1] The abbreviations used are: SR, sarcoplasmic reticulum; AMPPCP, adenosine 5′-[β,γ-methylene]triphosphate; AMPPNP, adenosine 5′-[β,γ-imido]triphosphate; caged nucleotide, P^3-1-(2-nitrophenyl)ethyl nucleotide; Ca_2E1, the calcium-ATPase complex with high affinity to Ca^{2+}; Ca_2E1NTP, the calcium-nucleotide-ATPase complex; Ca_2E1P, the ADP-sensitive phosphoenzyme; E2P, the ADP-insensitive phosphoenzyme; E2, the calcium-free ATPase with low affinity to Ca^{2+}; FTIR, Fourier transform infrared; N domain, the nucleotide binding domain; P domain, the phosphorylation domain; A domain, the actuator domain; t_b, the time constant of nucleotide binding; t_p, the time constant of ATPase phosphorylation; Δt_{NB}, the time interval of nucleotide binding spectra; Δt_{E1P}, the time interval of Ca_2E1P formation spectra; Ca_2E1 the calcium-ATPase complex with high affinity to Ca^{2+}.

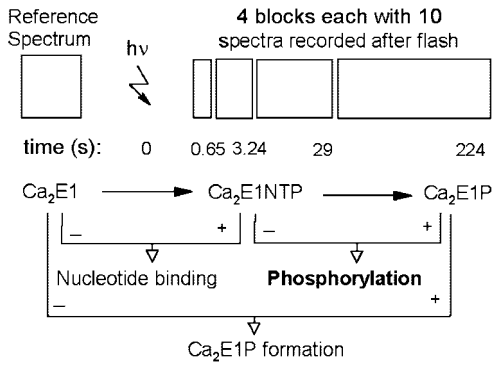

FIG. 1. **Reaction steps investigated here and the calculation of difference spectra.** The spectrum indicated with a *minus sign* was subtracted from the spectrum marked with a *plus sign*. The reference spectrum is with 300 scans; 4 blocks of spectra recorded after flash are with 1, 4, 40, and 300 scans, respectively. The ending time of each block is indicated (0.65, 3.24, 29, and 224 s).

EXPERIMENTAL PROCEDURES

Materials

SR vesicles were prepared as described (31). After a 60-min dialysis of 50 μl of SR vesicles in 100 ml of dialysis buffer (10 mM methylimidazole/HCl, pH 7.5, 200 μM $CaCl_2$, and 10 mM KCl), infrared samples were prepared by drying 15 μl of SR suspension on a CaF_2 window with a trough of 5-μm depth and 8-mm diameter and immediately rehydrating with ~0.8 μl of H_2O. The sample was sealed with a second flat CaF_2 window. The approximate sample composition based on 1 μl of sample volume is 1.2 mM Ca^{2+}-ATPase, 0.5 mg/ml Ca^{2+} ionophore (A23187), 150 mM methylimidazole, pH 7.5, 150 mM KCl, 10 mM $CaCl_2$, 10 mM dithiothreitol, 1 mg/ml adenylate kinase (except for ITP samples), and 10 mM caged nucleotide. Adenylate kinase, which regenerates ATP (2ADP → AMP + ATP), was added in samples with caged ATP and caged dATPs in order to repeat the kinetic experiments with one sample up to two times (12). Samples with caged ATP or caged 2′-dATP were also made in the absence of adenylate kinase for comparison. 10 mM Ca^{2+} was used instead of the physiological co-substrate Mg^{2+} to block the Ca_2E1P → E2P transition in order to achieve a maximum level of Ca_2E1P in the steady state after nucleotide release while slowing down the phosphorylation reaction (12, 32–34).

Apyrase (A6535 from Sigma) at low concentration (2 mg/ml) was used in some samples with caged ATP or caged ADP in the presence/absence of ATPase. Apyrase liberates inorganic phosphate from ATP and ADP: ATP → ADP + P_i → AMP + 2P_i. In the presence of ATPase apyrase consumes the ADP generated upon ATP hydrolysis. This leads to accumulation of the Ca_2E1P state without bound ADP. Although the affinity of ATPase to ATP is very high, apyrase should be used at low concentrations to avoid or slow down its reaction with ATP. Experiments in the absence of ATPase were done as control.

Control experiments with fluorescein isothiocyanate (35), thapsigargin (29), and AMPPNP (21) were performed, and it was confirmed that the infrared signals observed in our difference spectra were induced by reactions between nucleotide and the Ca^{2+}-ATPase.

Methods

FTIR Measurements—Time-resolved FTIR measurements of the Ca^{2+}-ATPase reaction were performed at 1 °C as described (12, 29). Photolytic release of nucleotides from the respective caged derivatives was triggered by a Xenon flash tube (N-185C, Xenon Corp., Woburn MA) for ATP and dATP or by a XeCl excimer laser for ITP (21). The number of photolysis flashes needed for saturating signals was determined as described (21). Data were acquired as shown in Fig. 1. A reference spectrum was first recorded with the protein in the Ca_2E1 state; after applying the photolysis flash(es), we recorded time-resolved infrared spectra with 65-ms time resolution from 0 to 225 s or longer. Difference spectra were obtained by subtracting the reference spectrum from the spectra recorded after nucleotide release. They reflect absorbance changes due to nucleotide binding and ATPase phosphorylation as well as the photolysis reaction under our experimental conditions. Groups or structures not involved in the reactions do not manifest in the difference spectra.

Kinetic Evaluation of Nucleotide Binding and Phosphorylation Reaction—The time constants of nucleotide binding (t_b), ATPase phosphorylation (t_p), and nucleotide hydrolysis were obtained by fitting the integrated band intensities of the marker bands at 1628 and 1641 cm^{-1} for nucleotide binding, at 1718, 1657, and 1549 cm^{-1} (at 1722 and 1707 cm^{-1} for 3′-dATP) for phosphorylation, and at 1241 cm^{-1} for nucleotide hydrolysis as described (12, 21, 36).

Calculation of Nucleotide Binding, Ca_2E1P Formation, and Phosphorylation Spectra—Nucleotide binding spectra show absorbance changes associated with the reaction Ca_2E1 → Ca_2E1NTP, and Ca_2E1P formation spectra show those associated with Ca_2E1 → Ca_2E1P. The time constants of t_b and t_p were used to determine the time intervals used to calculate the nucleotide binding spectra (Δt_{NB}) and Ca_2E1P formation spectra (Δt_{E1P}) as listed in Table I. We chose the time interval starting at $3t_b$ and ending at half of t_p for each nucleotide to calculate binding spectra. For obtaining Ca_2E1P formation spectra, we chose time intervals starting at $3t_p$ and ending at 68.1 s for ATP, ITP, and 2′-dATP, and for 3′-dATP ending at 224 s.

By subtracting the nucleotide binding spectrum from the Ca_2E1P formation spectrum, we obtained the phosphorylation spectrum showing the absorbance changes in the phosphorylation reaction (Ca_2E1NTP → Ca_2E1P) as shown in Fig. 1. Phosphorylation spectra show the spectral differences between the two time intervals, Δt_{NB} and Δt_{E1P}. Photolysis signals do not appear in phosphorylation spectra because they are identical in the nucleotide binding and the Ca_2E1P formation spectrum and are thus subtracted.

Difference spectra were normalized to a standard protein concentration (amide II absorbance 0.26) before averaging spectra from different samples to avoid the possible predominance of individual samples with high protein content in the averaged difference spectra, as described (29, 36). The number of averaged experiments and the amount of released nucleotides with different flash times are listed in Table I.

RESULTS

Phosphorylation with ATP—The phosphorylation spectrum obtained with ATP is shown in Fig. 2*A* (see also Table II). It reflects infrared absorbance changes in the reaction Ca_2E1ATP → Ca_2E1P. This spectrum is in agreement with those observed before (12, 36). Its band amplitude is three times smaller than that of the ATP binding spectrum, indicating smaller conformational changes in the phosphorylation step than upon nucleotide binding, in line with studies of FTIR spectroscopy (12), limited proteolysis (13), and crystal structures of complexes Ca_2E1AMPPCP and Ca_2E1ADP:AlF^{4-} (9, 10). Band assignments of the phosphorylation spectrum obtained with ATP have been discussed (36).

The phosphorylation spectrum obtained with ATP in the absence of adenylate kinase (data not shown) is very similar to that in the presence of adenylate kinase except that a larger band at 1241 cm^{-1} was observed compared with that obtained in the presence of adenylate kinase. The 1241 cm^{-1} band is due to a loss of one PO_2^- group upon ATP splitting,

$$\text{Adenosine-O-}PO_2^-\text{-}PO_2^-\text{-}PO_3^{2-} \rightarrow \text{adenosine-O-}PO_2^-\text{-}PO_3^{2-} + P_i \quad \text{(or } Ca_2\text{EIP)} \quad \text{(Eq. 1)}$$

This band has been assigned to the antisymmetric stretching mode (ν_{as}) of the PO_2^- of bound nucleotide (36). The smaller amplitude observed in the phosphorylation spectrum with ATP (Fig. 2) is due to the presence of adenylate kinase, which regenerates ATP.

Phosphorylation with 2′-dATP and ITP—Phosphorylation spectra obtained with 2′-dATP and with ITP are shown in Fig. 2, *A* and *B*. Double difference spectra in Fig. 2*C* show the difference between the phosphorylation spectrum obtained with 2′-dATP or ITP and that with ATP. We termed them extra conformational change spectra obtained with 2′-dATP or ITP as explained later.

In Fig. 2*A*, the phosphorylation spectrum with 2′-dATP shows signals similar to that with ATP except for the bands at ~1643, 1241, and 1115 cm^{-1}. The difference at ~1643 cm^{-1} in the amide I region is possibly due to different conformational changes of β-sheets during phosphorylation. In the presence of adenylate kinase, the 1241 cm^{-1} band obtained with ATP is

TABLE I
Parameters of spectra recording

Nucleotide	No. of experiments/no. of samples	Concentration of nucleotide/no. of flash	Time interval of nucleotide binding Δt_{NB}/Ca_2E1P formation Δt_{E1P}
ATP	23/12	3 mM/1 flash	0.46–0.90/5.84–68.1 s
2′-dATP	8/4	3 mM/1 flash	0.46–3.24/21.4–68.1 s
ITP	4/4	6.6 mM/3 flashes	0.72–3.32/26.7–68.1 s
3′-dATP	3/3	3 mM/1 flash	0.46–3.24/165–224.4 s
ATP (no ADK)	4/4	3 mM/1 flash	0.10–0.33/5.84–68.1 s

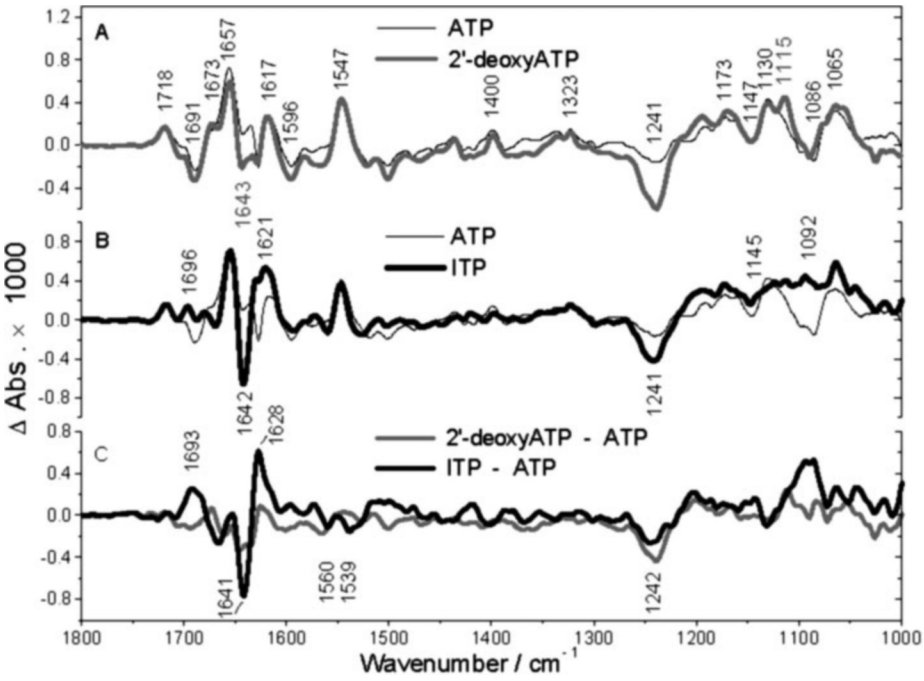

FIG. 2. *A*, phosphorylation spectra obtained with 3 mM ATP and 2′-dATP (1 °C, pH 7.5). The band positions are labeled in *black* for the spectrum with ATP and in *gray* for the spectrum with 2′-dATP. *B*, phosphorylation spectra obtained with 3 mM ATP and 6.6 mM ITP (1 °C, pH 7.5). The band positions are labeled in *black* for the spectrum with ITP. *C*, the extra conformational change spectra of 2′-dATP and of ITP. The band positions labeled in *black* are for the spectrum of ITP. Bands showing different amplitudes or positions observed in the phosphorylation spectra obtained with ATP or ATP analogs are listed in Table II.

TABLE II
Differences in the band amplitudes and positions in the phosphorylation spectra obtained with ATP and ATP analogues

Band Positions	Tentative band assignments	Nucleotide
cm^{-1}		
1696–1690	The amide I mode of β-sheet	ITP
1673	The amide I mode of turn	ITP
1657	The amide I mode of α-helices	3′-dATP
1645–1610	The amide I mode of β-sheet	ITP, 2′-dATP, 3′-dATP
1241	The $\nu_{as}(PO_2^-)$ mode of the bound nucleotide	ITP, 2′-dATP, 3′-dATP

smaller than that obtained with 2′-dATP as shown in Fig. 2*A*. However, with ATP in the absence of adenylate kinase, this band shows the same integrated band intensity and kinetic change as with 2′-dATP in the presence of adenylate kinase. Thus, we attribute the difference between ATP and 2′-dATP in the presence of adenylate kinase to faster regeneration of ATP from ADP as compared with that of 2′-dATP from 2′-dADP. Samples with 2′-dATP in the absence of adenylate kinase were made to investigate this further, and we observed no difference (data not shown) compared with 2′-dATP samples in the presence of adenylate kinase. Adenylate kinase was recently found to use ADP more efficiently than 2′-dADP (37). But in an earlier study the efficiency was very similar for ADP and 2′-dADP (38). Here our observation agrees with the most recent result (37). With ITP (no adenylate kinase present), the band amplitude at 1241 cm^{-1} (Fig. 2*B*) is similar to that in the phosphorylation spectrum obtained with ATP in the absence of adenylate kinase.

As shown in Fig. 2*B* the phosphorylation spectrum obtained with ITP is significantly different from those obtained with ATP and with 2′-dATP. The differences compared with ATP are particularly pronounced in the amide I region. Larger band amplitudes indicate that larger conformational changes occur when ITP phosphorylates the ATPase. Bands at 1696, 1642, and 1621 cm^{-1} in the amide I region of the phosphorylation spectrum obtained with ITP are different from those with ATP. They indicate different conformational changes of β-sheets or turns in the phosphorylation reaction with ITP.

In the following we will explore the characteristics of this extra conformational change upon phosphorylation with ITP. A spectrum of the extra conformational change is shown in Fig. 2*C*. This spectrum was calculated by subtracting the phosphorylation spectrum obtained with ATP from that obtained with ITP. In Fig. 3*A* this spectrum is compared with the spectra of ATP and ITP binding. As the figure shows, the extra conformational change spectrum with ITP is very similar in shape to the nucleotide binding spectra. A similar shape indicates a similar character of the conformational change, *i.e.* that secondary structure elements are perturbed in a similar manner. This indicates that conformational changes characteristic of ATP binding take place during phosphorylation with ITP. The band amplitudes in the extra conformational change spectrum are between those of ITP binding and ATP binding. This indicates that the extent of the extra conformational change is larger than that of ITP binding

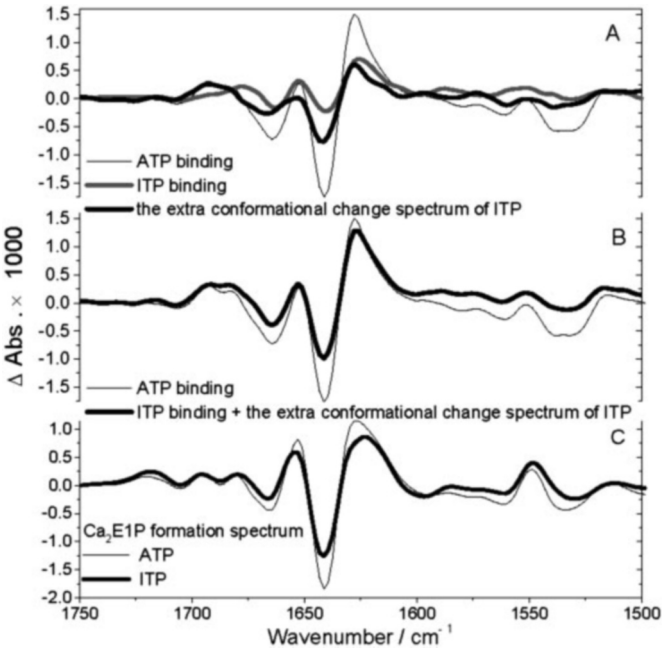

FIG. 3. *A*, comparison of the ATP binding spectrum, the ITP binding spectrum, and the extra conformational change spectrum obtained with ITP (*black line* in Fig. 2*C*). *B*, comparison of the ATP binding spectrum and the sum of ITP binding spectrum and extra conformational change spectrum with ITP. *C*, comparison of the Ca_2E1P formation spectra obtained with ATP and ITP.

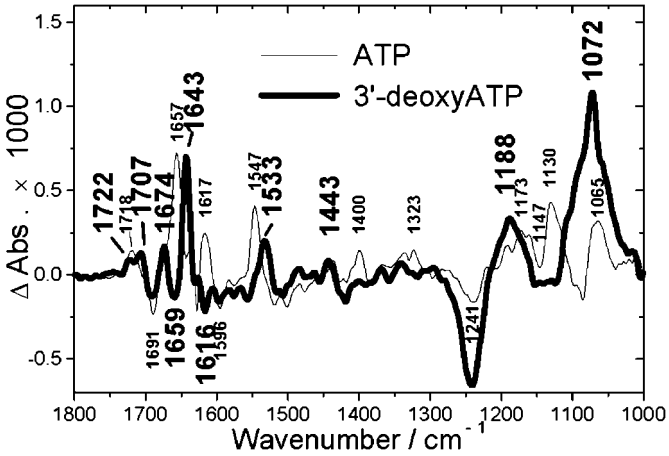

FIG. 4. **Comparison of the phosphorylation spectrum obtained with ATP and the spectrum obtained with 3′-dATP by subtracting the 3′-dATP binding spectrum from the spectrum averaged from 165.4 to 224 s.** The band positions labeled in *small black type* are for the spectrum with ATP and in *larger black type* are for the spectrum with 3′-dATP.

but smaller than that of ATP binding. Fig. 3*A* also shows that the extent of conformational change upon ITP binding is only about 30% that of ATP binding (21) as judged from the amplitude of the main bands. Because we can expect that the initial state in our samples is the same for all nucleotides, the different amplitudes in the binding spectra indicate a different structure of the nucleotide ATPase complexes as shown previously (21). However, if the extra conformational change spectrum with ITP is added to the ITP binding spectrum, the resulting spectrum has ~70% of the amplitude of the ATP binding spectrum (as judged from the band amplitudes of the two largest bands). This comparison is shown in Fig. 3*B*. The generated spectrum is in fact very similar in shape and amplitude to the 2′-dATP binding spectrum (21), which has about two times larger band amplitudes than the ITP binding spectrum. This indicates that if the extra conformational change upon phosphorylation with ITP had taken place already upon ITP binding, the structure of the ITP ATPase complex would be very similar to that obtained with 2′-dATP and more similar to that with ATP than actually observed.

The consequence of the extra conformational change upon phosphorylation with ITP is that the conformation of Ca_2E1P obtained with ITP becomes more similar to that obtained with ATP in comparison to the nucleotide ATPase complexes with ITP and ATP. This is evident from the relatively similar band amplitudes of the Ca_2E1P formation spectra with ITP and ATP (see Fig. 3*C* and Ref. 21) as compared with the large amplitude differences in the nucleotide binding spectra (see Fig. 3*A* and Ref. 21). The Ca_2E1P formation spectrum with ITP is very similar to that obtained with 2′-dATP (21).

Phosphorylation with 3′-dATP—Absorption changes after 3′-dATP binding were also observed as shown in Fig. 4. The spectrum obtained with 3′-dATP differs from the other phosphorylation spectra (Fig. 2) in that it shows different band positions and amplitudes for most of the bands. The spectrum with 3′-dATP does not show the marker band for phosphorylation at 1718 cm^{-1} observed with ATP and other ATP analogs. Instead, there are two bands at 1722 and 1707 cm^{-1}. The bands at 1674, 1643, and 1533 cm^{-1} in the amide I region indicate that conformational changes occurred after binding. A band characteristic of ATP splitting is also observed at 1241 cm^{-1} with 3′-dATP.

Despite the differences to the other phosphorylation spectra, we tentatively attribute this spectrum with 3′-dATP to phosphorylation of the ATPase for the following reasons. (i) It is known that 3′-dATP can phosphorylate the ATPase, although to a lower extent compared with ATP (39); (ii) there are bands at 1722 and 1707 cm^{-1} close to the marker band of phosphorylation at 1718 cm^{-1}; (iii) the conformational changes after 3′-dATP binding are accompanied by 3′-dATP consumption as indicated by the negative band at 1241 cm^{-1}, which exhibits the same slow kinetic change as the band at 1722 cm^{-1} (Fig. 5).

The absorbance changes after 3′-dATP binding are very slow; reaction kinetics of the bands at 1722, 1707, and 1241 cm^{-1} observed with 3′-dATP (t = 52, 61, and 55 s, respectively) were ~30-fold slower than those with ATP (t_p = 2 s). The time course of these bands is shown in Fig. 5. The absorption changes are only partly complete during the measuring time of our experiments. The difference spectrum shown in Fig. 4 was obtained by subtracting the 3′-dATP binding spectrum from the spectrum averaged from 165.4 to 224 s. This spectrum shows ~80% of the absorbance changes associated with the complete reaction (calculated from the fitting of the bands at 1722 and 1707 cm^{-1}).

Kinetics of the Conformational Change—Kinetic evaluation of the bands at 1657 or 1643 cm^{-1} in the amide I region and at 1547 or 1533 cm^{-1} in the amide II region (data not shown) give the time constants of the conformational change of the protein backbone. For all nucleotides the time constants are the same as those of the marker band for enzyme phosphorylation at 1718 cm^{-1} (at 1722 cm^{-1} for 3′-dATP). The 1718 cm^{-1} band has been assigned to the C═O stretching vibration of aspartyl phosphate on the basis of model compound studies (36). This shows that the conformational change of the protein backbone proceeds with the same velocity as phosphorylation at Asp-351.

Effects of ADP on Ca_2E1P Conformation—To determine the effect of bound ADP on Ca_2E1P conformation, ADP was removed by a helper enzyme, apyrase. Apyrase experiments were done with caged ADP and caged ATP in the presence/absence of the ATPase. In control experiments without ATPase there were no significant signals observed in the

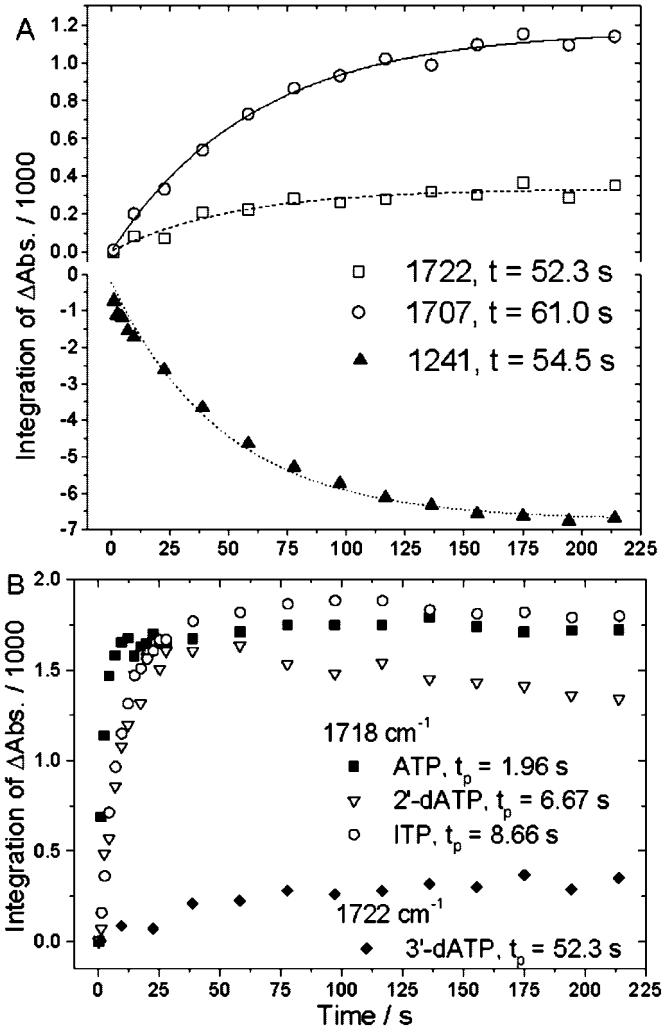

FIG. 5. *A*, kinetics of bands at 1722, 1707, and at 1241 cm^{-1} in the experiments with 3′-dATP. *B*, comparison of kinetics at the 1718 or 1722 cm^{-1} band for phosphorylation with ATP, ITP, 2′-dATP, and 3′-dATP.

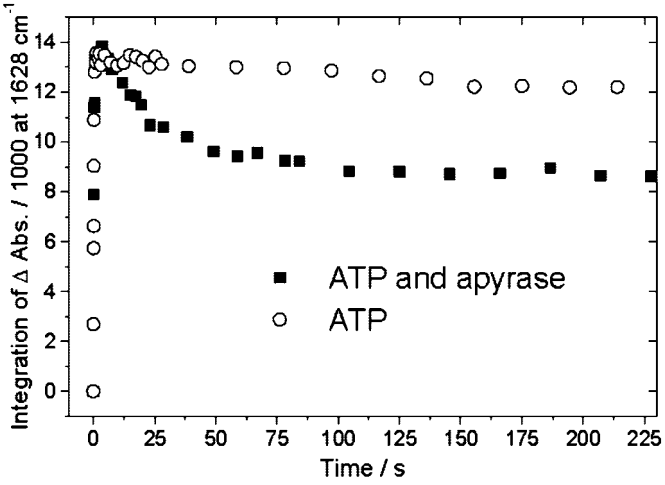

FIG. 6. **Kinetics of the 1628 cm^{-1} band in the experiments with ATP in the presence/absence of apyrase.** The integration was done with respect to a base line drawn between two points that were the average of data points between 1643 and 1638 as well as 1611 and 1607 cm^{-1}. This gives a similar measure of the extent of conformational change as the one we have used before (21).

amide I region with both ATP and ADP, which indicates that ATP or ADP interacting with apyrase does not induce observable absorbance changes at the apyrase concentration used. Therefore, the presence of apyrase will not disturb absorbance changes due to conformational changes of the ATPase. In samples that contain apyrase and ATPase, ATP or ADP binding to the ATPase and ATPase phosphorylation with ATP were observed with the same extent of conformational change and the same reaction rates as without apyrase. However, the largest bands at 1641 and 1628 cm^{-1} in the amide I region decay to 70% after phosphorylation with ATP or decay to nearly zero after ~16 s in experiments of ADP binding, whereas they are constant in the absence of apyrase. For the ATP experiments we evaluated the kinetics of the 1641 and 1628 cm^{-1} bands by integrating the 1628 cm^{-1} band with respect to a base line that includes the negative 1641 cm^{-1} band (see the legend of Fig. 6). The result of integration, therefore, reports on both bands, which were used to quantify the extent of conformational change (21). The time course of the 1628 cm^{-1} band area is shown in Fig. 6. In the absence of apyrase, the band area increases upon ATP binding (within 0.1 s) and remains constant after phosphorylation with ATP (after 2 s). Its time constants on binding and phosphorylation are not affected by the presence of apyrase. But with apyrase the band area decays by 30% after phosphorylation with a time constant of ~20 s, which was also observed for ADP consumption by apyrase in experiments using caged ADP with or without ATPase. At the same time the marker band of phosphorylation at 1718 cm^{-1} remains constant, indicating that the phosphoenzyme level retains constant. We, therefore, attribute the decay of infrared signals in the amide I region to dissociation of ADP from Ca_2E1P, which is irreversible in the presence of the ADP-consuming apyrase. Thus, dissociation of ADP relaxes the conformation of Ca_2E1P partially back toward Ca_2E1.

DISCUSSION

The Conformational Change Observed by Infrared Spectroscopy—Previously we have estimated that the net change in secondary structure involves up to 10 amino acids for all partial reactions of the SR Ca^{2+}-ATPase (12). The net change upon nucleotide binding was substantial and comparable with those of Ca^{2+} binding and phosphoenzyme conversion. Changes observed upon phosphorylation were smaller but of the same order of magnitude, in line with very similar structures found for a nucleotide-ATPase complex and a Ca_2E1P analogue (9, 10). With the availability of structures for Ca_2E1 and the ATPase complex with AMPPCP, the value of 10 residues for a net change of secondary structure can now be scrutinized. We analyzed the structures with a modified Kabsch and Sander algorithm (40) as implemented in the program ICMLite and considered the secondary structure types, helical structures, β-strand, and others. The number of residues involved in a net secondary structure change between the 1EUL entry for the Ca_2E1 structure and the 1T5S entry for Ca_2E1AMPPCP (9) was surprisingly high, 47. However, performing the same analysis with the more recent structure 1SU4 of Ca_2E1, the number was considerably lower, 6. This discrepancy is mainly due to a considerable reassignment of coil residues in 1EUL to helical residues in 1SU4. In fact, the number or residues involved in a net change of secondary structure between the two Ca_2E1 structures 1EUL and 1SU4 is 46, about as large as that between the Ca_2E1 1EUL structure and the Ca_2E1AMPPCP 1T5S structure. Because of its higher resolution we chose the 1SU4 structure for Ca_2E1 to explore differences between 1SU4 and structures for Ca_2E1AMPPCP, 1T5S (9) and molecules A and B of Protein Data Bank entry 1VFP (10). The number of residues involved in a net change of secondary structure are 6, 15, and 8, respectively, which is similar to the differ-

ences observed between the 3 Ca_2E1AMPCP structures where the number is 3–10. Because infrared spectroscopy can detect only a net change in a structure, many individual compensating changes will not be revealed. In fact, the actual number of residues undergoing a change between the secondary structure types considered is larger; that is, 54–77 residues for the Ca_2E1 (1SU4) to Ca_2E1AMPPCP transition. This discussion indicates that (i) the net change in secondary structure between Ca_2E1 and Ca_2E1AMPPCP is very small and is correctly estimated by infrared spectroscopy (12) and that (ii) caution should be applied when structures are chosen to calibrate infrared spectra for secondary structure analysis. Secondary structure algorithms will give different secondary structure contents depending on resolution and crystallization conditions.

In our previous work (21) we have tentatively attributed most of the amide I signals (1700–1610 cm^{-1}) to the N-P hinge region. There we discussed that our infrared spectra will not reflect the N-P hinge movement directly because we assumed the hinge region to be flexible. Instead we anticipated that hinge movements will reflect indirectly in infrared spectra due to conformational changes in adjacent well structured regions. However, a recent NMR study (41) on the isolated N domain of Na^+, K^+-ATPase showed that the N-P hinge region has a defined conformation. Therefore, movements in the N-P hinge region might well reflect directly in infrared spectra.

The prominent band near 1628 cm^{-1} in our nucleotide binding spectra (Fig. 3) (21) and in the extra conformational change spectrum obtained with ITP (Fig. 2*C*) will not be caused by the N-P hinge region. Such low wavenumber bands are due to β-sheets with a considerable number of parallel or antiparallel strands. The spectral position is sensitive to the number of aligned strands and the planarity of the sheets (for antiparallel β-sheets) but is nearly independent to the number of residues per strand (42–44). There are three extended β-sheets in the Ca^{2+}-ATPase, one in each of the N, A, and P domains. In the following we will tentatively attribute the 1628 cm^{-1} and the adjacent 1641 cm^{-1} band to a structural change of the β-sheet in the P domain. The N domain moves as a rigid body in the transition from Ca_2E1 to Ca_2E1AMPPCP (10); thus, its β-sheet is not expected to contribute significantly to the band at 1628 cm^{-1}. The β-sheet in the A domain gains six residues in the transition as revealed by a secondary structure analysis of Ca_2E1 (1SU4) and all available Ca_2E1AMPPCP structures. This, however, will not lead to a change in absorbance near 1628 cm^{-1} since the additional residues are in β-sheet sections with only 2 antiparallel strands.

Most interesting is the observation that the β-sheet of P domain alters its structure and acts as a secondary hinge (10), in line with the view that the P domain should not be regarded as a rigid body (45). These changes are expected to reflect in infrared spectra as discussed in the following. In Ca_2E1AMPPCP a short section of this sheet has 8 parallel strands comprising 2 residues per strand and a total number of 16 residues. The strands are connected by two lines of hydrogen bonding along residues 653–675/676–623/624–350/351–701/702–718/719–733/734–332 and 651–675/674–623/622–350/349–701/700–718/717–733/732–334. In Ca_2E1 the first line of hydrogen bonding is disrupted between the fourth and fifth strand (between residues 351 and 701; N-O distance increases from 2.7 to 5.7 Å), which effectively splits the β-sheet here into two parts. The second line of hydrogen bonding is disrupted in Ca_2E1 between the seventh and eighth strand (between residues 732 and 334; N-O distance increases from 2.8 to 3.9 Å), which narrows the β-sheet by one strand and weakens between the fourth and fifth strand (between residues 349 and 701; N-O distance increases from 2.8 to 3.2 Å). Disruption of hydrogen bonding will also disrupt the transition dipole coupling between these residues, which is the main determinant of the spectral position in the infrared spectrum.

The main consequence for infrared absorption is that transition dipole coupling between the two parts of the β-sheet is weaker in Ca_2E1, which will make the infrared absorption more like that of two β-sheets with four parallel strands. Thus, the P domain β-sheet is expected to absorb at higher wavenumber in Ca_2E1 than in Ca_2E1AMPPCP. In line with this we observe a negative band at 1641 cm^{-1} and a positive band at 1628 cm^{-1} upon nucleotide binding (21), and we tentatively attribute a considerable portion of these bands to the change in β-sheet structure of the P domain.

Effects of the Adenine Ring of ATP on Phosphorylation—Differences between phosphorylation spectra obtained with ATP and with ITP are larger than those between phosphorylation spectra obtained with ATP and 2′-dATP (Fig. 2). However, a similar phosphorylation reaction rate and the same extent of Ca_2E1P accumulation were obtained with ITP and 2′-dATP (21), which indicates that the extent of conformational change is not an important factor for these properties.

Interestingly, Scofano *et al.* (46) observed an overshoot of phosphorylation with 1 mM ITP but not with 5 μM ATP (pH 7.4, room temperature, 0.1 mM $CaCl_2$, 1.0 mg/ml leaky vesicles). However, a similar steady state level of phosphoenzyme was obtained with 5 μM ATP and 1 mM ITP, and the same amount of phosphoenzyme formation with ITP or GTP as with ATP was observed at high Ca^{2+} concentration (47, 48). Our results are partly consistent with these observations. In our study the accumulation of the Ca_2E1P state with 6.6 mM ITP and 3 mM ATP is similar. However, an overshot of phosphorylation is not observed with ITP because the amplitude of the marker band at 1718 cm^{-1} in the phosphorylation spectrum obtained with ITP is the same as that with ATP.

In the phosphorylation spectrum obtained with ITP, additional signals in the amide I region (Fig. 2*C*) were observed, which are similar to nucleotide binding signals as shown in Fig. 3*A*. Several explanations are in principle possible for the larger bands observed in the phosphorylation spectrum obtained with ITP as follows.

Nucleotide binding might be slow with ITP so that there is a convolution of binding and phosphorylation spectra. This can be excluded from the kinetic evaluation discussed before (21). The time constants for binding and phosphorylation with ITP are 0.23 and 8.66 s, respectively. The nucleotide-ATPase complex and the phosphoenzyme with ITP are even better separated in time than with ATP. The slow phase of the bands at 1628 and 1641 cm^{-1} (where the main differences with respect to ATP are observed) has the same rate as the phosphorylation marker band at 1718 cm^{-1} (data not shown).

In ITP samples, ~6.6 mM ITP was released, ~3.6 mM more than in ATP samples. The additional bands in the amide I region of the phosphorylation spectrum of ITP could be due to the extra amount of ITP interacting with the ATPase in the phosphorylation reaction. However, in samples with 3 mM released ITP, a phosphorylation spectrum with a similar shape was observed (data not shown), showing that the extra amount of ITP has no influence on the appearance of the additional bands in the ITP phosphorylation spectrum. In addition, ITP was found not to bind to the regulatory site of the ATPase (49).

A fraction of ATPase could exist in dimers or higher oligomers that allow ITP to bind only to one of the ATPase molecules. Phosphorylation of this molecule then allows ITP to bind to the second ATPase molecule followed by rapid phosphorylation. One would then have to assume that ATP binding is not governed by this allosteric effect, although the ATP bind-

ing-induced conformational changes are similar in character to those induced by ITP.

The most likely explanation is that larger conformational changes occur upon phosphorylation with ITP. In the proceeding step of the reaction cycle, the conformational change induced by ITP binding is smaller than that induced by ATP binding (21). As discussed above the extra conformational change with ITP during phosphorylation is similar to that upon nucleotide binding. If the extra conformational changes occurring during phosphorylation with ITP occurred in the ITP binding reaction, the conformational changes would be very similar to those occurring upon 2′-dATP binding (Fig. 3*B*). The 1628 cm^{-1} band was tentatively attributed above to the secondary hinge movement of the β-sheet in the P domain. Therefore, our phosphorylation spectrum with ITP indicates that this β-sheet hinge movement is promoted upon phosphorylation by ITP but not by the other nucleotides used.

In line with our result, a fluorescence study (50) showed also that a fluorescence change observed for ATP binding was not observed for ITP binding but later for phosphorylation by ITP. Transient interactions during phosphorylation might be responsible for the extra conformational change with the result that the enzyme snaps into the closed conformation. For 2′-dATP and ATP this conformational change is largely induced upon binding. Thus, it seems that upon phosphorylation with ITP the enzyme catches up on a conformational change that cannot be achieved by ITP binding because the interactions between protein and base moiety are impaired. Analysis of crystal structures of Ca_2E1AMPPCP (9, 10) shows that Glu-442 is close to the adenine amino group. This residue will repulse the negative partial charge on the inosine oxygen. This may explain the weaker binding of ITP and the smaller extent of conformational change upon ITP binding (21). After ATPase phosphorylation with ITP, IDP may dissociate from the phosphoenzyme under our conditions, which will relieve the repulsion, resulting in extra conformational change upon phosphorylation with ITP.

Effects of the Ribose OH Groups of ATP on Phosphorylation—The crystal structure of Ca_2E1AMPPCP (10) shows that the ribose 2′-OH interacts by van der Waals contacts with the N domain but not with the P domain. Arg-678 and Arg-560 may interact electrostatically with the negative partial charge on the oxygen of 2′-OH. This may explain the effect of 2′-OH modification on binding and phosphorylation rate (21). The phosphorylation spectra of ATP and 2′-dATP are very similar. This demonstrates that 2′-OH has little impact on the conformational change upon phosphorylation. Small differences are evident in the extra conformational change spectrum shown in Fig. 2*C*. The extra conformational change spectrum of 2′-dATP is similar to that of ITP in shape, but the band amplitudes are considerably smaller. This indicates that there are also extra conformational changes occurring with 2′-dATP upon enzyme phosphorylation, although their extent is much smaller than for ITP.

In our previous study (21) we inferred that Ca_2E1P could not be formed from 3′-dATP because there was no clear marker band at 1718 cm^{-1} for Ca_2E1P formation. In this work, however, the kinetic analysis reveals slow absorbance changes that we attribute to the phosphorylation reaction as discussed under "Results."

The ribose 3′-OH is important for enzyme phosphorylation since 3′-dATP has unique properties, it phosphorylates the ATPase very slowly (t_p = 54 s), its phosphorylation spectrum is very different from the other nucleotides, and its Ca_2E1P formation spectrum (data not shown) exhibits only very small absorbance changes in the amide I region. This implies that the Ca_2E1P conformation obtained with 3′-dATP is more similar to that of Ca_2E1 than to Ca_2E1P obtained with ATP. Thus, the hinge between the N and P domain will be as open after phosphorylation with 3′-dATP as before, *i.e.* the phosphoenzyme would not adopt the closed conformation, as obtained with ATP. Phosphorylation might not require the closed conformation since non-nucleotide substrates like acetyl phosphate can also phosphorylate the ATPase but may not be able to link N and P domain upon binding.

It was found (39) that 3′-NH_2-ATP was utilized in a manner equivalent to ATP. The 3′-NH_2 group is similar to the 3′-OH group as a donor of hydrogen bonds, whereas the 3′-H group is an acceptor of a hydrogen bond. The similar results obtained with 3′-NH-ATP and ATP and the differences observed with 3′-dATP and ATP can, therefore, be explained by the 3′-OH group forming a hydrogen bond (39), which was found to be with the β-phosphate in the crystal structure of Ca_2E1AMPPCP (9). This hydrogen bond stabilizes a bend conformation of the triphosphate chain, helping stabilize the AMPPCP-ATPase complex for the subsequent enzyme phosphorylation (9). Crystal structures of Ca_2E1AMPPCP (9, 10) also show that the 3′-OH interacts with Arg-678 of the P domain, which appears to form hydrogen bonds with residues both in the N and P domains. The position of Arg-678 is such that the 3′-OH hydrogen is directed toward the β-phosphate. Our infrared results agree with these crystal structures and point out the importance of the 3′-OH on enzyme phosphorylation. Its existence and interaction with other groups seem to be prerequisites for the closed conformation upon nucleotide binding (21) and for fast phosphorylation.

Previously, the rate of phosphorylation of the Ca^{2+}-ATPase was found to decrease by more than one order of magnitude with 2′-dATP and 3′-dATP (39). We also observed slower phosphorylation with the two dATPs, but the extent of decreased phosphorylation rate was less (~4-fold) with 2′-dATP.

Effect of ADP on Phosphoenzyme Conformation—The results obtained in our apyrase experiments in the presence of ATP and the ATPase elucidate the ADP effect on the conformation of Ca_2E1P. With the helper enzyme apyrase, ADP dissociation from the phosphoenzyme Ca_2E1P is irreversible because apyrase removes ADP. ADP dissociation reverses some of the conformational changes of nucleotide binding with the effect that Ca_2E1P conformation is more similar to the Ca_2E1 conformation without ADP than with bound ADP (Fig. 6). We, therefore, conclude that ADP binds to Ca_2E1P, which promotes the closed conformation of the phosphoenzyme. After phosphorylation with ITP or 2′-dATP, IDP or 2′-dADP seems not to have such an effect on Ca_2E1P conformation as ADP. Ca_2E1P without bound ADP may adopt a defined more open conformation of the cytoplasmic domains, or the equilibrium between closed and open conformation is more on the open side than with bound ADP.

Conclusions—Our results demonstrate that infrared spectroscopy can be used to probe ligand-protein interactions. In the particular case of phosphorylation of the SR Ca^{2+}-ATPase, modifications at the 2′-OH, 3′-OH, and amino group of ATP affect phosphorylation of the Ca^{2+}-ATPase by affecting the conformational change of the protein backbone and by slowing down the reaction velocity. Conformational changes upon phosphorylation are characteristic of the nucleotide used as shown by the different phosphorylation spectra obtained with different nucleotides. This indicates that interactions of the ATP molecule distant from the phosphate groups contribute to approaching the γ-phosphate to the phosphorylation site Asp-351 and/or to forming the phosphate binding pocket; the functional groups 2′-OH and 3′-OH and the adenine ring of ATP are

important for inducing the conformational change of the ATP-ATPase complex that is competent for phosphoryl transfer. Therefore, phosphorylation is an interactive process in which the formation of interactions of the γ-phosphate is reinforced by interactions of other ATP groups, which can be at the opposite end of the ATP molecule.

Acknowledgments—W. Mäntele (Institut für Biophysik, Johann Wolfgang Goethe-Universität) is gratefully acknowledged for use of their facilities. We thank W. Hasselbach (Max-Planck-Institut, Heidelberg) for the gift of Ca^{2+}-ATPase, and J. E. T. Corrie (National Institute for Medical Research, London) and F. von Germar for help in the preparation of caged compounds. We thank a reviewer for valuable suggestions on the role of ADP.

REFERENCES

1. Hasselbach, W., and Makinose, M. (1961) *Biochem. Z.* **333,** 518–528
2. Hasselbach, W. (1974) in *The Enzymes* (Boyer, P. D., ed) 3rd Ed., pp. 431–467, Academic Press, Inc., New York
3. Makinose, M., and The, R. (1965) *Biochem. Z.* **343,** 383–393
4. Toyoshima, C., and Inesi, G. (2004) *Annu. Rev. Biochem.* **73,** 269–292
5. McIntosh, D. B. (2000) *Nat. Struct. Biol.* **7,** 532–535
6. Kendrew, J., and Lawrence, E., eds (1994) *The Encyclopedia of Molecular Biology*, 1st Ed., p. 624, Blackwell Science, Oxford
7. Toyoshima, C., Nakasako, M., Nomura, H., and Ogawa, H. (2000) *Nature* **405,** 647–655
8. Toyoshima, C., and Nomura, H. (2002) *Nature* **418,** 605–611
9. Sorensen, T. L. M., Moller, J. V., and Nissen, P. (2004) *Science* **304,** 1672–1675
10. Toyoshima, C., and Mizutani, T. (2004) *Nature* **430,** 529–535
11. Hua, S., Inesi, G., Nomura, H., and Toyoshima, C. (2002) *Biochemistry* **41,** 11405–11410
12. Barth, A., von Germar, F., Kreutz, W., and Mäntele, W. (1996) *J. Biol. Chem.* **271,** 30637–30646
13. Danko, S., Yamasaki, K., Daiho, T., Suzuki, H., and Toyoshima, C. (2001) *FEBS Lett.* **505,** 129–135
14. Colthup, N. B., Daly, L. H., and Wiberley, S. E. (1990) *Introduction to Infrared and Raman Spectroscopy*, 3rd Ed., Academic Press, Inc., New York
15. Siebert, F. (1995) *Methods Enzymol.* **246,** 501–526
16. Cantor, C. R., and Schimmel, P. R. (1980) *Biophysical Chemistry. Part II: Techniques for the Study of Biological Structure and Function*, pp. 466–480, W. H. Freeman and Co., New York
17. Goormaghtigh, E., Cabiaux, V., and Ruysschaert, J. M. (1994) *Subcell. Biochem.* **23,** 329–362
18. Barth, A., and Zscherp, C. (2002) *Q. Rev. Biophys.* **35,** 369–430
19. Cepus, V., Scheidig, A. J., Goody, R. S., and Gerwert, K. (1998) *Biochemistry* **37,** 10263–10271
20. Granjon, T., Vacheron, M.-J., Vial, C., and Buchet, R. (2001) *Biochemistry* **40,** 2988–2994
21. Liu, M., and Barth, A. (2003) *J. Biol. Chem.* **278,** 10112–10118
22. Griffiths, P. R., and de Haseth, J. A. (1986) *Fourier Transform Infrared Spectrometry*, John Wiley & Sons, New York
23. Wharton, C. W. (2000) *Nat. Prod. Rep.* **17,** 447–453
24. Arrondo, J. L. R., Muga, A., Castresana, J., and Goñi, F. M. (1993) *Prog. Biophys. Mol. Biol.* **59,** 23–56
25. Jackson, M., and Mantsch, H. H. (1995) *Crit. Rev. Biochem. Mol. Biol.* **30,** 95–120
26. Braiman, M. S., and Rothschild, K. J. (1988) *Annu. Rev. Biophys. Biophys. Chem.* **17,** 541–570
27. Jung, C. (2000) *J. Mol. Recognit.* **13,** 325–351
28. Liu, M., and Barth, A. (2002) *Biospectroscopy* **67,** 267–270
29. Liu, M., and Barth, A. (2003) *Biophys. J.* **85,** 3262–3270
30. Kaplan, J. H., Forbush, B., and Hoffman, J. F. (1978) *Biochemistry* **17,** 1929–1935
31. De Meis, L., and Hasselbach, W. (1971) *J. Biol. Chem.* **246,** 4759–4763
32. Suzuki, H., Nakamura, S., and Kanazawa, T. (1994) *Biochemistry* **33,** 8240–8246
33. Shigekawa, M., Wakabayashi, S., and Nakamura, H. (1983) *J. Biol. Chem.* **258,** 8698–8707
34. Lacapere, J.-J., and Guillain, F. (1990) *J. Biol. Chem.* **265,** 8583–8589
35. Barth, A., Mäntele, W., and Kreutz, W. (1991) *Biochim. Biophys. Acta* **1057,** 115–123
36. Barth, A., and Mäntele, W. (1998) *Biophys. J.* **75,** 538–544
37. Resnick, S. M., and Zehnder, A. J. B. (2000) *Appl. Environ. Microbiol.* **66,** 2045–2051
38. Ladner, W. E., and Whitesides, G. M. (1985) *J. Org. Chem.* **50,** 1076–1079
39. Coan, C., Amaral, J. A., and Verjovski-Almeida, S. (1993) *J. Biol. Chem.* **268,** 6917–6924
40. Kabsch, W., and Sander, C. (1983) *Biopolymers* **22,** 2577–2637
41. Hilge, M., Siegal, G., Vuister, G. W., Guntert, P., Bloor, S. M., and Abrahams, J. P. (2003) *Nat. Struct. Biol.* **10,** 468–474
42. Chirgadze, Y. N., and Nevskaya, N. A. (1976) *Biopolymers* **15,** 627–636
43. Chirgadze, Y. N., and Nevskaya, N. A. (1976) *Biopolymers* **15,** 607–625
44. Kubelka, J., and Keiderling, T. A. (2001) *J. Am. Chem. Soc.* **123,** 12048–12058
45. Reuter, N., Hinsen, K., and Lacapere, J. J. (2003) *Biophys. J.* **85,** 2186–2197
46. Scofano, H. M., Vieyra, A., and De Meis, L. (1979) *J. Biol. Chem.* **254,** 10227–10231
47. de Meis, L., and de Mello, M. C. F. (1973) *J. Biol. Chem.* **248,** 3691–3701
48. Souza, D. O. G., and de Meis, L. (1976) *J. Biol. Chem.* **251,** 6355–6359
49. Petretski, J. H., Wolosker, H., and De Meis, L. (1989) *J. Biol. Chem.* **264,** 20339–20343
50. Kubo, K., Suzuki, H., and Kanazawa, T. (1990) *Biochim. Biophys. Acta* **1040,** 251–259